

MODEL-BASED 3D MICRO-NAVIGATION AND BATHYMETRY ESTIMATION FOR INTERFEROMETRIC SYNTHETIC APERTURE SONAR

Benjamin Thomas^a, Alan Hunter^a, Samantha Dugelay^b

^aUniversity of Bath, Claverton Down, Bath, BA2 7AY, UK

^bNATO STO CMRE, Viale S. Bartolomeo, 400, 19126 La Spezia SP, IT

Contact author: Benjamin Thomas, b.w.thomas@bath.ac.uk

Abstract: *Sub-wavelength navigation information is vital for the formation of all synthetic aperture sonar (SAS) data products. This challenging requirement can be achieved using the redundant phase centre (RPC) or displaced phase centre antenna (DPCA) micro-navigation algorithm, which uses cross-correlation of signals with inter-ping coherence to estimate time delays and hence make navigation estimates. In this paper a new approach to micro-navigation for interferometric synthetic aperture sonar is introduced. The algorithm makes 3D vehicle position estimates for each sonar ping by making use of time delays measured between all possible pairs of redundant phase centre arrays, using both interferometric arrays on each side of the vehicle. Simultaneous estimation of coarse bathymetry allows the SAS images to be projected onto ground-range. The method is based on non-linear minimization of the difference in modelled and measured time delays and surges between redundant phase centre arrays. The approach is demonstrated using data collected by the CMRE MUSCLE AUV using its 270-330 kHz SAS during the MANEX'14 experiment. SAS images have been projected onto the coarsely estimated bathymetry, and interferograms have been formed. The coarse bathymetry estimate and vehicle navigation estimate are validated by the quality of the image focussing and the near-zero phase of the interferogram. The method has the potential to improve through-the-sensor navigation aiding and to increase the accuracy of single-pass bathymetry estimation. Future development of the algorithm for repeat-pass operation has the potential to enable repeat-pass track registration in three dimensions. The method is therefore an important step towards improved coherent change detection and high resolution bathymetry estimation.*

Keywords: *Synthetic Aperture Sonar, Micro-navigation, Interferometry*

1. INTRODUCTION

Synthetic aperture sonar (SAS) is an advanced acoustic imaging technology capable of imaging sea-floor swathes of hundreds of meters with centimetre-scale resolution. The coherent processing requires the trajectory of the sonar to be known to within a fraction of a wavelength. This requirement can be achieved using the redundant phase centre (RPC) or displaced phase centre antenna (DPCA) micro-navigation algorithm [1]. RPCs are overlapping portions of the virtual monostatic array used to approximate the true bi-static geometry of multi-receiver SAS.

The RPC micro-navigation algorithm utilizes time delays measured between signals received by RPC arrays to make navigation estimates. However, in reality these time delays are also a function of bathymetry and medium fluctuations. Isolation of this ‘triad of confounding factors’ [2] enables accurate estimation of vehicle navigation and sea-floor bathymetry.

Many SAS-equipped autonomous underwater vehicles (AUVs) have a pair of vertically separated receiver arrays on each side of the vehicle. Typically, the RPC micro-navigation algorithm is applied to only one array per side, with independent measurements sway and surge made at multiple range windows. The navigation estimates are used to generate images for each pair of arrays, and the interferogram formed between the image pairs is used to generate bathymetry estimates. However, this two-stage process may incompletely isolate the phase contributions from navigation and bathymetry, which may corrupt their estimates. Developments to RPC micro-navigation have included heave estimation using dual-sided SAS [3], [4]. However, these make a flat bathymetry assumption and hence the navigation estimates may contain bathymetry-induced errors.

This paper describes a one-stage simultaneous micro-navigation and coarse bathymetry estimation technique for single-pass interferometric SAS. The method involves least-squares minimization of the difference between measured and modelled time delays and surges between RPC arrays. The method leverages the mutual information contained in the time delay estimates made at all range windows between all possible inter-ping and intra-ping (interferometric) RPC pairs. A similar technique was demonstrated in earlier preliminary work [2], where time delays measured between inter-pass RPC arrays on a single side of the vehicle were used to estimate inter-pass array displacements in sway and heave between individual pairs of pings of different passes. However, in that work the vehicle paths were not estimated due to the absence of coupling between adjacent pings. In the current work, coupling between pings is achieved by introducing measured and modelled surge between RPC arrays into the method, which allows estimation of the vehicle path.

The technique is demonstrated using data collected by the CMRE MUSCLE AUV using its 270-330 kHz SAS during the MANEX’14 experiment. The new method has been used to make estimates of vehicle navigation and coarse bathymetry. SAS images are formed onto the coarse bathymetry estimate, which is validated by forming interferograms between the image pairs.

2. MICRO-NAVIGATION METHOD

The new micro-navigation method is based upon a non-linear least-squares minimization of measured and modelled surges and time delays between RPC arrays. The use of all of the available surges and time delays between RPC array pairs allows the vehicle translations in surge, sway and heave to be measured from the sonar data, while at the same time making a coarse bathymetry estimate. The angular rotations of the vehicle in roll, pitch and yaw are measured by the inertial navigation system (INS). Fig. 1a shows the possible pairs of RPC arrays between which surge and time delays can be measured on each side of the vehicle, for an interferometric SAS. This shows that measurements of four inter-array surges and six inter-array time delays can be made per side, ping and range window. The fusion of all of these measurements enables simultaneous 3D micro-navigation and bathymetry estimation.

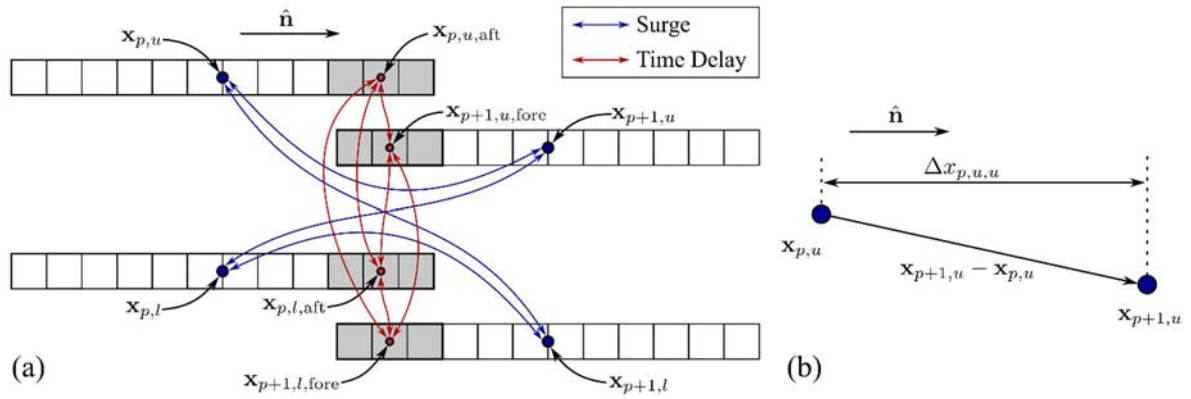


Fig. 1 – (a) Overlapping phase centre arrays between subsequent pings. Arrows join the pairs of phase centre arrays between which surges and time delays are measured. (b) Modelled surge between the upper phase centre arrays of two pings.

2.1. Surge Measurement and Modelling

The received signals are short-time windowed, producing signals corresponding to small range windows. Surge measurement is performed using the method described in [3] at every range window. Cross-correlation of the windowed signals is performed for a number of candidate surge values, corresponding to integer multiples of the distance between phase centres. Interpolation using a quadratic kernel is then used to refine each estimate. Finally, a weighted mean of the surge estimates at all range windows gives the inter-array surge.

The modelled inter-array surge is the length of the projection of the vector between two array centres in the direction of the platform orientation. For example, the modelled surge between the upper array of ping p and the upper array of ping $p + 1$ is given by

$$\Delta x_{p,u,u} = \|(\mathbf{x}_{p,u} - \mathbf{x}_{p+1,u}) \cdot \hat{\mathbf{n}}_p\|, \quad (1)$$

as shown in Fig. 1b, where $\mathbf{x}_{p,u}$ and $\mathbf{x}_{p+1,u}$ denote the modelled position of the centre of the upper phase centre array on pings p and $p + 1$ respectively, and

$$\hat{\mathbf{n}}_p = \begin{pmatrix} \cos(\psi_p) & -\sin(\psi_p) & 0 \\ \sin(\psi_p) & \cos(\psi_p) & 0 \\ 0 & 0 & 1 \end{pmatrix} \begin{pmatrix} \cos(\phi_p) & 0 & \sin(\phi_p) \\ 0 & 1 & 0 \\ -\sin(\phi_p) & 0 & \cos(\phi_p) \end{pmatrix} \begin{pmatrix} 1 \\ 0 \\ 0 \end{pmatrix}, \quad (2)$$

is the modelled platform orientation on ping p , where ψ_p and ϕ_p are the yaw and pitch of the vehicle on ping p .

2.2. Time Delay Measurement and Modelling

Measurement of the time delay between signals received by RPC arrays is achieved by finding the maximum of their cross-correlation function. The time delay measurements are split into an integer number of phase cycles, plus a fraction of a phase cycle. Care must be taken to ensure that any errors in the phase cycle number estimate are detected and corrected [5].

The complexity of the time delay model must be chosen depending on the application. Here we consider a model which does not employ the phase centre assumption i.e. propagation paths are modelled from the transmitter to the sea-floor and back to the receiving transducers. However, the stop-and-hop assumption is used, which assumes that the vehicle is stationary while the signal is transmitted and received, and then moves instantly to the position of the next ping. This has been shown to be a reasonable assumption for the MUSCLE AUV [6].

Consider the fore-most upper array elements of ping p and the aft-most upper array elements of ping $p + 1$ that collect coherent signals due to the overlap of their corresponding phase centres. The locations of the centres of these sub-arrays are denoted by $\mathbf{x}_{p,u,fore}$ and $\mathbf{x}_{p+1,u,aft}$ respectively. The positions of the transmitter on pings p and $p + 1$ are denoted by $\mathbf{x}_{tx,p}$ and $\mathbf{x}_{tx,p+1}$ respectively. Consider a modelled location on the sea-floor $\mathbf{x}_{f,p}$, which is constrained to lie on the plane passing through $\mathbf{x}_{p,mid}$ with normal vector $\hat{\mathbf{n}}_p$, where

$$\mathbf{x}_{p,mid} = (\mathbf{x}_{p,u,fore} + \mathbf{x}_{p+1,u,aft} + \mathbf{x}_{tx,p} + \mathbf{x}_{tx,p+1})/4 \quad (4)$$

is the mid-point of the RPC arrays formed by pings p and $p + 1$.

Two-way travel times from the transmitter, to the sea-floor location, and back to the redundant elements of the receiving arrays for pings p and $p + 1$ are given by (5) and (6), where c is the medium propagation speed.

$$t_{p,u,fore} = (\|\mathbf{x}_{tx,p} - \mathbf{x}_{f,p}\| + \|\mathbf{x}_{p,u,fore} - \mathbf{x}_{f,p}\|)/c \quad (5)$$

$$t_{p+1,u,aft} = (\|\mathbf{x}_{tx,p+1} - \mathbf{x}_{f,p}\| + \|\mathbf{x}_{p+1,u,aft} - \mathbf{x}_{f,p}\|)/c \quad (6)$$

The difference in modelled two-way travel times for this pair of RPC arrays is then given by

$$\Delta t_{p,u,fore,p+1,u,aft} = t_{p+1,u,aft} - t_{p,u,fore} \quad (7)$$

2.3. Least-squares minimization

The coarse bathymetry and navigation estimates are generated by minimizing the differences between modelled and measured time delays and surges. On each iteration, the models for inter-array surges and time delays are linearized about the current navigation and bathymetry estimate. The linearized model is then solved to estimate updated vehicle and sea-floor positions. This process is iterated until convergence is achieved, and results in 3D estimates of the vehicle position for each ping and a coarsely sampled point-cloud of bathymetry estimates.

3. RESULTS

The new simultaneous micro-navigation and bathymetry estimation method has been applied to data collected by the CMRE MUSCLE AUV using its 270-330 kHz SAS during the MANEX'14 experiment. The vehicle was programmed to follow a straight line at a constant distance above the sea-floor with a speed of 1.4 m/s. SAS images have been generated using the navigation estimated by the new method, onto the coarse bathymetry estimate. The resulting navigation estimates from the new method are compared with those measured by the on-board navigation hardware in Fig. 2.

The smoothly-varying micro-navigation estimate in Fig. 2a follows a similar shape to that measured by the navigation hardware. The difference between the navigation hardware and micro-navigation estimates appears to arise from an integrated constant sway rate offset. However, it is not possible to attribute the error to either the navigation hardware or the micro-navigation estimate. Fig. 2c shows the sway rates, which shows that the navigation hardware estimates are severely quantised, whereas the micro-navigation estimates vary smoothly. The vehicle depth estimated by the micro-navigation method in Fig. 2b also varies smoothly, but seems to decrease slightly more rapidly than the measurement made by the depth sensor. This could be due to incorrectly modelled sonar mounting position on the platform, an incorrect sound speed assumption, or inaccurate sonar calibration. The depth rates shown in Fig. 2d show severe quantisation of the depth sensor, while the micro-navigation estimate varies smoothly.

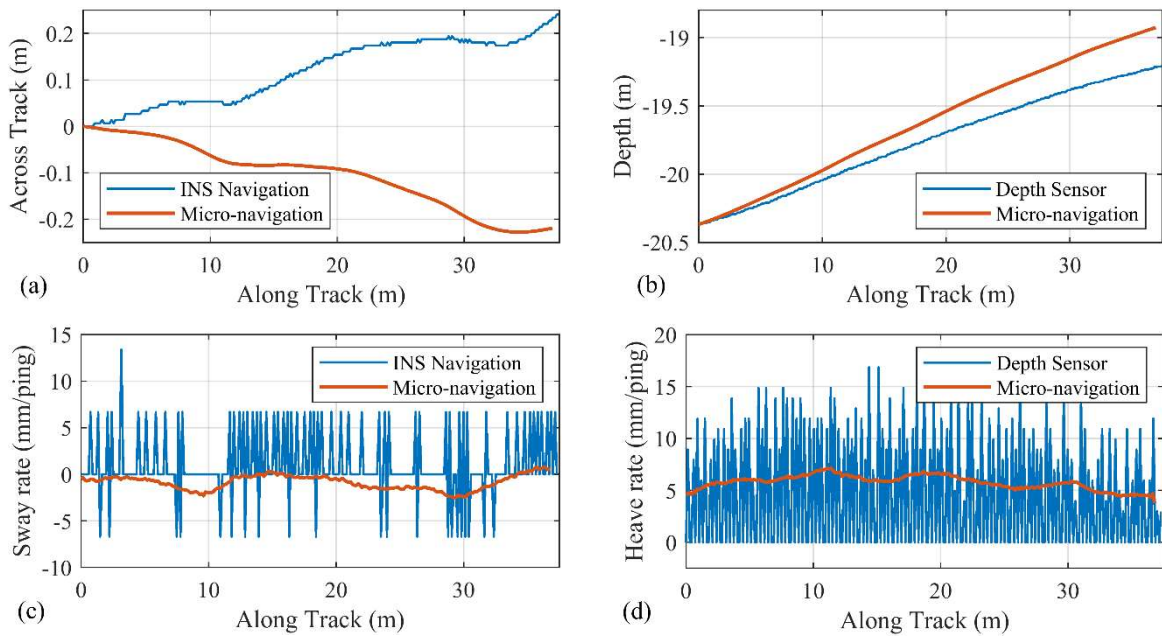


Fig. 2 – (a) Vehicle path (b) Vehicle depth (c) Sway rate (d) Heave rate, estimated by the navigation hardware and the new micro-navigation method.

The port-side SAS image projected onto the coarse bathymetry estimate is shown in Fig. 3. The scene is predominantly gently sloping and includes a pipe and concrete blocks. Colour encodes the deviation of the coarse bathymetry estimate from the best-fitting plane through the coarse bathymetry. This reveals some scouring around the proud objects.

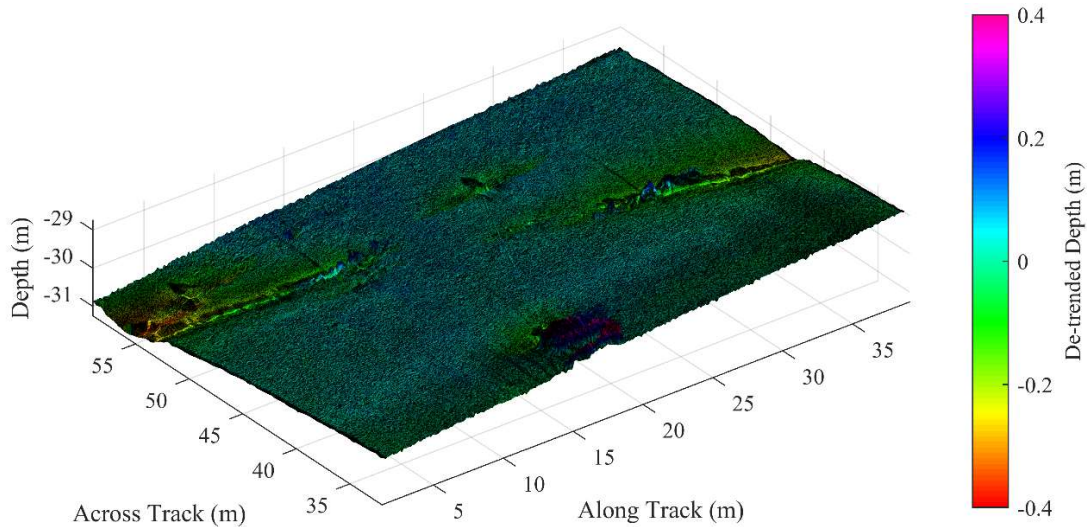


Fig. 3 – SAS image on coarse bathymetry. Colour encodes deviation from sloping plane.

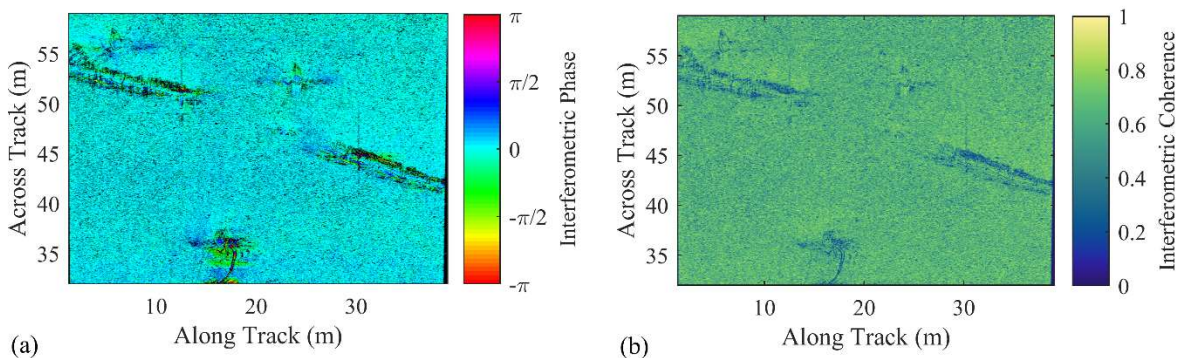


Fig. 4 – Interferogram (a) phase (b) magnitude

The interferogram formed between images generated from the upper and lower arrays is shown in Fig. 4. Zero interferogram phase indicates that the estimated bathymetry is accurate. The result shows near-zero phase over most of the scene, deviating only in high complexity regions. The phase of the interferogram could be used to improve the coarse bathymetry estimate. The interferogram magnitude is high, suggesting that the images are well registered.

4. CONCLUSION AND FURTHER WORK

Simultaneous 3D micro-navigation and bathymetry estimation for single-pass InSAS has been demonstrated using data collected by the CMRE MUSCLE AUV using its 270-330 kHz SAS during the MANEX'14 experiment. It is not possible to compare the navigation estimate against ground-truth. However, the focussed images, the near-zero interferometric phase and the high interferometric coherence validate the navigation and coarse bathymetry estimates.

The isolation of navigation and bathymetry information achieved by the new method has the potential to improve vehicle navigation estimation and the quality of single-pass interferometric bathymetry estimates. Further work will involve estimation of fine bathymetry using the single-pass interferogram. Additionally, estimation of medium propagation speed and fusion of measurements from the navigation hardware will be included in the method, potentially improving through-the-sensor navigation aiding [7]. The method will also be developed for repeat-pass SAS operations, which has the potential to improve coherent change detection and enable much higher resolution bathymetry estimation.

5. ACKNOWLEDGEMENTS

The authors would like to thank the Centre for Maritime Research and Experimentation for the MANEX'14 data and the Autonomous Mine Countermeasures team scientists, engineers and the crew of NRV Alliance for their support in collecting the data. The trial and CMRE's work are funded by the NATO Allied Command Transformation.

REFERENCES

- [1] D. Billon and F. Fohanno, "Theoretical performance and experimental results for synthetic aperture sonar self-calibration," *IEEE Ocean. Eng. Soc. Ocean. Conf. Proc. (Cat. No.98CH36259)*, vol. 2, pp. 965–970, 1998.
- [2] B. Thomas, A. J. Hunter, and S. Dugelay, "Repeat-pass micro-navigation and bathymetry estimation using interferometric synthetic aperture sonar," in *IOA Synthetic Aperture Sonar and Synthetic Aperture Radar*, 2018.
- [3] D. A. Cook, "Synthetic Aperture Sonar Motion Estimation and Compensation," Georgia Institute of Technology, 2007.
- [4] H. Schmaljohann *et al.*, "Dual-sided micronavigation for synthetic aperture sonar," in *1st International Conference and Exhibition on Underwater Acoustics*, 2013, pp. 119–126.
- [5] S. Leier, "Signal processing techniques for seafloor ground-range imaging using synthetic aperture sonar systems," Technische Universität Darmstadt, 2014.
- [6] Y. Pailhas, S. Dugelay, and C. Capus, "Impact of temporal Doppler on synthetic aperture sonar imagery," *J. Acoust. Soc. Am.*, vol. 143, no. 1, pp. 318–329, 2018.
- [7] W. A. Connors, A. J. Hunter, and J. Dillon, "Increasing Navigation Effectiveness in GPS Denied Environments Using Through-The-Sensor SAS Techniques," in *4th International Conference on Synthetic Aperture Sonar and Synthetic Aperture Radar 2018*, 2018, pp. 99–106.